

RESEARCH ARTICLE

10.1002/2015GB005160

Key Points:

- Fires reduced terrestrial carbon sink by $0.57 \text{ Pg C yr}^{-1}$ during 1901–2010
- The declining trend of pyrogenic carbon emissions reversed since the mid-1980s
- Pyrogenic carbon emissions per unit burned area increased in recent decades

Supporting Information:

- Figures S1–S5

Correspondence to:

H. Tian,
tianhan@auburn.edu

Citation:

Yang, J., H. Tian, B. Tao, W. Ren, C. Lu, S. Pan, Y. Wang, and Y. Liu (2015), Century-scale patterns and trends of global pyrogenic carbon emissions and fire influences on terrestrial carbon balance, *Global Biogeochem. Cycles*, 29, 1549–1566, doi:10.1002/2015GB005160.

Received 31 MAR 2015

Accepted 23 AUG 2015

Accepted article online 25 AUG 2015

Published online 30 SEP 2015

©2015. The Authors.

This is an open access article under the terms of the Creative Commons Attribution-NonCommercial-NoDerivs License, which permits use and distribution in any medium, provided the original work is properly cited, the use is non-commercial and no modifications or adaptations are made.

Century-scale patterns and trends of global pyrogenic carbon emissions and fire influences on terrestrial carbon balance

Jia Yang¹, Hanqin Tian¹, Bo Tao¹, Wei Ren¹, Chaoqun Lu¹, Shufen Pan¹, Yuhang Wang², and Yongqiang Liu³

¹International Center for Climate and Global Change Research, School of Forestry and Wildlife Sciences, Auburn University, Auburn, Alabama, USA, ²School of Earth and Atmospheric Science, Georgia Institute of Technology, Atlanta, Georgia, USA,

³Center for Forest Disturbance Science, USDA-Forest Service, Athens, Georgia, USA

Abstract Fires have consumed a large amount of terrestrial organic carbon and significantly influenced terrestrial ecosystems and the physical climate system over the past century. Although biomass burning has been widely investigated at a global level in recent decades via satellite observations, less work has been conducted to examine the century-scale changes in global fire regimes and fire influences on the terrestrial carbon balance. In this study, we investigated global pyrogenic carbon emissions and fire influences on the terrestrial carbon fluxes from 1901 to 2010 by using a process-based land ecosystem model. Our results show a significant declining trend in global pyrogenic carbon emissions between the early 20th century and the mid-1980s but a significant upward trend between the mid-1980s and the 2000s as a result of more frequent fires in ecosystems with high carbon storage, such as peatlands and tropical forests. Over the past 110 years, average pyrogenic carbon emissions were estimated to be $2.43 \text{ Pg C yr}^{-1}$ ($1 \text{ Pg} = 10^{15} \text{ g}$), and global average combustion rate (defined as carbon emissions per unit area burned) was $537.85 \text{ g C m}^{-2}$ burned area. Due to the impacts of fires, the net primary productivity and carbon sink of global terrestrial ecosystems were reduced by $4.14 \text{ Pg C yr}^{-1}$ and $0.57 \text{ Pg C yr}^{-1}$, respectively. Our study suggests that special attention should be paid to fire activities in the peatlands and tropical forests in the future. Practical management strategies, such as minimizing forest logging and reducing the rate of cropland expansion in the humid regions, are in need to reduce fire risk and mitigate fire-induced greenhouse gases emissions.

1. Introduction

Fire plays a vital role in terrestrial ecosystem dynamics as well as the Earth's climate system [Bowman *et al.*, 2009; Randerson *et al.*, 2006; Rogers *et al.*, 2013; Ward *et al.*, 2012]. Biomass burning emits large amounts of greenhouse gases, such as carbon dioxide (CO_2), methane (CH_4), and nitrous oxide (N_2O), into the atmosphere, and then modifies atmospheric components and radiation budget [Kaiser *et al.*, 2012; Langmann *et al.*, 2009; van der Werf *et al.*, 2010; Wiedinmyer *et al.*, 2011; Tian *et al.*, 2015]. It has been indicated that interannual variation in global fire emissions is one of the major factors in controlling atmospheric CO_2 and CH_4 growth rates [Bousquet *et al.*, 2006; van der Werf *et al.*, 2004]. Moreover, fire can substantially affect land-atmosphere interactions by altering terrestrial vegetation types and land surface albedo [Jin *et al.*, 2012; Liu, 2005a, 2005b; Lyons *et al.*, 2008]. Meanwhile, fires are strongly influenced by climate and weather conditions [Bowman *et al.*, 2009; Rogers *et al.*, 2015; van der Werf *et al.*, 2008a, 2008b; Westerling *et al.*, 2006]. For example, it has been recognized that precipitation is negatively correlated with fire activities in the humid regions with abundant fuels (such as tropical rainforest) but positively correlated with fire activities in the arid regions with lower fuel loading where higher precipitation during vegetation growing season could stimulate fire activities by increasing the amount of fuels in the following fire season [van der Werf *et al.*, 2008a].

At a global level, the recent estimates of terrestrial carbon sink clustered at around 2.6 Pg C yr^{-1} [e.g., Poulter *et al.*, 2014; Le Quéré *et al.*, 2013], while estimates of global pyrogenic carbon emissions in recent years clustered at around 2.0 Pg C yr^{-1} [e.g., Kaiser *et al.*, 2012; Li *et al.*, 2014; van der Werf *et al.*, 2010]. Global pyrogenic carbon emissions show substantial year-to-year variations, varying from more than 2.5 Pg C yr^{-1} in the two El Niño years 1997 and 1998 to lower than 1.6 Pg C yr^{-1} in 2001 and 2009 [van der Werf *et al.*, 2010].

Therefore, the interannual variation in pyrogenic carbon emissions is a major contributor to changes in the terrestrial carbon sink. To evaluate the contribution of fires to land carbon balance, it is necessary to consider both the direct pyrogenic carbon emissions and carbon dynamics during postfire vegetation regrowth. Although a large portion of fire emissions can be counteracted by the postfire vegetation regrowth in many terrestrial ecosystems (such as Canadian boreal forest and Amazon tropical forest), fire has been recognized as one of the most critical factors controlling the overall direction of carbon fluxes between land and the atmosphere [Bond-Lamberty *et al.*, 2007; Gatti *et al.*, 2014].

Fire emissions and impacts have been extensively studied in many regions across the globe in the context of climate change and intensified human activities [e.g., Andela and van der Werf, 2014; Kasischke and Turetsky, 2006; Mack *et al.*, 2011; Westerling *et al.*, 2006]. The earliest estimation of global fire carbon emissions dates back to the 1980s [Seiler and Crutzen, 1980]. However, global fires and their influences on terrestrial carbon balance prior to the satellite era are largely unknown. Up to date, various approaches have been used to investigate burned area and fire emissions. Generally, methods of investigating global burned area could be classified into three categories, i.e., ground-based inventory data interpolation [Mouillot and Field, 2005; Schultz *et al.*, 2008], satellite observation [Giglio *et al.*, 2013; Roy *et al.*, 2008; Tansey *et al.*, 2008], and model simulation [e.g., Li *et al.*, 2012; Pechony and Shindell, 2009; Thonicke *et al.*, 2010; Yang *et al.*, 2014a; Yue *et al.*, 2014b]. Global fire emissions can be either estimated based on burned area, fuel loading, and combustion completeness [e.g., Mouillot *et al.*, 2006; Prentice *et al.*, 2011; Thonicke *et al.*, 2010; van der Werf *et al.*, 2010] or derived directly through satellite-observed fire radiative power [Kaiser *et al.*, 2012; Zhang *et al.*, 2014].

To examine fire impacts on terrestrial ecosystems, fire exclusion field experiments that compare sites with different fire management strategies have been implemented in many regions [e.g., Bowman and Panton, 1995; Moreira, 2000; Tilman *et al.*, 2000]. All of these experiments indicated that the long-term fire exclusion practices can lead to increases in forest coverage and carbon accumulation in vegetation and soil. Meanwhile, numerical model simulations show that tree coverage and vegetation biomass may decrease linearly with increasing burned area [Poulter *et al.*, 2015]. The closed forest coverage is projected to increase from 27% to 56% of vegetated land area under fire exclusion scenario [Bond *et al.*, 2005]. Terrestrial ecosystem carbon storage can be fundamentally modified by fires. It has been found that the land-based carbon sink in the northern high latitudes was weakened by wildfires in recent decades [Hayes *et al.*, 2011]. However, the role of fire in the global carbon balance are largely unknown. Recently, land ecosystem models (such as Community Land Model-fire model [Li *et al.*, 2014], Organizing Carbon and Hydrology in Dynamic Ecosystems model [Yue *et al.*, 2014a], and Lund-Potsdam-Jena model [Poulter *et al.*, 2015]) have been applied to investigate global fire emissions and fire impacts on terrestrial ecosystems. All of these studies designed “fire-on” and “fire-off” numerical experiments and computed the differences in carbon balance between the two experiments. It is worth noting that the estimated reductions in the terrestrial carbon sink present substantial variation among these studies. Li *et al.* [2014] showed that the fire-induced reduction in carbon sink is 1.0 Pg C yr^{-1} ; Yue *et al.* [2014a] suggested that the reduction is $0.32 \text{ Pg C yr}^{-1}$, while Poulter *et al.* [2015] reported that global net biome production is relatively insensitive to fires. The discrepancies can be largely attributed to the differences in the estimation of pyrogenic carbon emission and the potential carbon sequestration during postfire regrowth processes. To better address the legacy effect of historical fires on carbon balance which is highly related to postfire regrowth processes, it is necessary to examine terrestrial carbon dynamics over long time period, such as decades and centuries [Tian *et al.*, 2012a]. At a global level, century-scale burned area data sets have been reconstructed based on fire inventory data [Mouillot and Field, 2005] or process-based simulations in combination with satellite observations [Yang *et al.*, 2014a]. In this study, we used a process-based land ecosystem model, the Dynamic Land Ecosystem Model (DLEM) [Tian *et al.*, 2015], in combination with a newly developed burned area data set [Yang *et al.*, 2014a] and other gridded environmental data sets to investigate global pyrogenic carbon emissions and the role of fire in terrestrial carbon fluxes during 1901–2010. The specific objectives of this study are (1) to provide a century-scale estimation of global pyrogenic carbon emissions; (2) to evaluate the role of fire in the terrestrial carbon budget; and (3) to discuss the influences of climate, human activities, and atmospheric components on the changing trend of historical biomass burning and their future implications.

Table 1. Parameter Table of Combustion Completeness and Tree Mortality Used in This Study^a

Vegetation Types	Combustion Completeness (%)					Tree Mortality (%)
	Leaf	Stem	Root	Litter	Coarse Woody Debris	
BBDF	80	30	5	95	30	70
BNEF	80	30	5	95	30	70
BNDF	80	30	5	95	30	70
TBDF	80	30	5	95	30	70
TBEF	80	30	5	95	30	70
TNEF	80	30	5	95	30	70
TNDF	80	30	5	95	30	70
TrBDF	50	20	5	95	30	60
TrBEF	80	30	5	95	30	70
Shrub	90	30	5	95	30	50
C3 grass	95	-	5	95	-	-
C4 grass	95	-	5	95	-	-

^aNote that BBDF stands for boreal broadleaf deciduous forest; BNEF stands for boreal needleleaf evergreen forest; BNDF stands for boreal needleleaf deciduous forest; TBDF stands for temperate broadleaf deciduous forest; TBEF stands for temperate broadleaf evergreen forest; TNEF stands for the temperate needleleaf evergreen forest; TNDF stands for the temperate needleleaf deciduous forest; TrBDF stands for tropical broadleaf deciduous forest; TrBEF stands for the tropical broadleaf evergreen forest.

2. Method and Data

2.1. The Dynamic Land Ecosystem Model (DLEM)

The DLEM is a process-based land biosphere model, which mainly simulates the fluxes and storages of carbon, nitrogen, and water in terrestrial ecosystems as influenced by multiple environmental factors, such as climate, atmospheric components, land use/cover changes, and various disturbances [Tian *et al.*, 2011]. Recently, we have coupled a process-based fire submodule into the DLEM to investigate burned area and fire emissions at both regional and global scales [Yang *et al.*, 2014a].

In this study, we mainly describe the model parameterizations regarding fire-induced carbon emissions and forest mortality. The details of other processes (such as carbon, nitrogen, water cycles, and their coupling) are available in our previous publications [Chen *et al.*, 2013; Chen *et al.*, 2012; Liu *et al.*, 2013; Lu and Tian, 2013; Lu *et al.*, 2012; Pan *et al.*, 2014; Ren *et al.*, 2011; Tao *et al.*, 2014; Tian *et al.*, 2014; Yang *et al.*, 2014a, 2014b]. In the DLEM, available fuels include vegetation biomass (leaf, stem, and root), litter, coarse woody debris, and soil organic carbon. Carbon emissions during biomass burning (C_{bt} , $g C m^{-2}$) at grid level are estimated as

$$C_{bt} = \sum_{ipft=1}^4 \sum_{ifuel=1}^5 (C_{ipft, ifuel} CC_{ipft, ifuel} BF_{ipft} f_{ipft}) + f_{peatfire} Depth_{fire} Dens_{peat} \quad (1)$$

where $ipft$ is the index of natural vegetation types within one model grid (DLEM allows a maximum of four natural vegetation types coexisting in one grid); $ifuel$ is the index of fuel types (1—leaf, 2—stem, 3—root, 4—litter, and 5—coarse woody debris); BF_{ipft} is the monthly burned fraction of each natural vegetation type (%), which is assumed to be equal to burned fraction at grid level; f_{ipft} is the fraction of biome in the grid (%); $C_{ipft, ifuel}$ is the DLEM-simulated fuel loading of each fuel type ($g C m^{-2}$); and $CC_{ipft, ifuel}$ is the combustion completeness (%), which can either be estimated based on the input burn severity data set or retrieved from vegetation specific parameter table (Table 1).

Peatlands with shallow water table are difficult to be ignited. However, in recent decades, the frequency and extent of peat fires increased associated with drying up of peatlands due to climate warming and human activities [Turetsky *et al.*, 2015; Hooijer *et al.*, 2010]. For example, forest plantation (such as oil palm and pulpwood) in recent decades reduced forest canopy, drained the water in peatlands, and enhanced fire risks in the tropics. In this study, we assume no tropical peat fires until the large-scale agricultural development occurred in recent three decades [Hooijer *et al.*, 2010]. For fires in peatlands, burned depth ($Depth_{fire}$, cm) is estimated for tropical peatlands and boreal peatlands, respectively. In tropical peatlands, $Depth_{fire}$ is computed according to soil water content: the maximum value is set at 51 cm when soil water is lower than wilting point and the minimum is at 15 cm when soil moisture is higher than field capacity. Carbon density

($Dens_{peat}$) is set to $570 \text{ g C m}^{-2} \text{ cm}^{-1}$, which is similar to the field measurements of Southeast Asian peatlands in 1997 [Page *et al.*, 2002]. For the boreal peatlands, $Depth_{fire}$ (13.1 cm) and the $Dens_{peat}$ ($269.3 \text{ g C m}^{-2} \text{ cm}^{-1}$) are taken from the measurements in Turetsky *et al.* [2011]. Peatland area used in this study is estimated as the overlapped area of peatlands in Yu *et al.* [2010] and the wetland in the Global Lakes and Wetlands Database [Lehner and Döll, 2004]. Burned fraction in peatlands at grid level ($f_{peatfire}$) is set to the minima of grid burned fraction and peatland fraction.

In the DLEM, we explicitly consider fire-induced tree mortality. After fire events, a fraction of trees are killed and the dead plant tissues transfer to their corresponding dead carbon pools (i.e., litter pool and woody debris pool).

$$C_{mort_{ipft, leaf \rightarrow agl}} = BF_{ipft} C_{ipft, leaf} (1 - CC_{ipft, leaf}) Mort_{ipft} \quad (2a)$$

$$C_{mort_{ipft, stem \rightarrow agCWD}} = BF_{ipft} C_{ipft, stem} (1 - CC_{ipft, stem}) Mort_{ipft} \quad (2b)$$

$$C_{mort_{ipft, froot \rightarrow bgl}} = BF_{ipft} C_{ipft, froot} (1 - CC_{ipft, froot}) Mort_{ipft} \quad (2c)$$

$$C_{mort_{ipft, croot \rightarrow bgCWD}} = BF_{ipft} C_{ipft, croot} (1 - CC_{ipft, croot}) Mort_{ipft} \quad (2d)$$

where C_{mort} is the carbon density (g C m^{-2}) of living biomass killed by fires; $leaf \rightarrow agl$, $stem \rightarrow agCWD$, $froot \rightarrow bgl$, and $croot \rightarrow bgCWD$ denote the transfer of killed leaf, killed stem, killed fine root, and killed coarse root to aboveground litter pool, aboveground coarse woody debris pool, belowground litter pool, and belowground coarse woody debris pool, respectively; and $Mort_{ipft}$ is the fire-induced tree mortality rate (%). Similar to the parameterization of combustion completeness, fire mortality in the DLEM can be either derived from satellite-based burn severity index when satellite information is available or derived from vegetation specific parameter table (Table 1). In this study, we simply used the second approach to estimate combustion completeness and forest mortality owing to the lack of long-term burn severity information worldwide. The DLEM also considers the tree age-related changes in ecosystem productivity and forest coverage during postfire vegetation recovery. Associated processes have been documented elsewhere [Chen *et al.*, 2013].

2.2. Model Input Data Sets

Gridded, georeferenced data sets are compiled from various sources to drive the DLEM at the spatial resolution of $0.5^\circ \times 0.5^\circ$, including climate (daily mean/maximum/minimum temperature, precipitation, downward solar radiation, and relative humidity), atmospheric CO_2 concentration, nitrogen deposition, land use/cover change, burned area, topography, soil texture, and other ancillary data sets [Tian *et al.*, 2015]. Additional details regarding data availability are described in the supporting information. Temporal variations in global temperature, precipitation, CO_2 concentration, and nitrogen deposition rates are illustrated in Figure S1 in the supporting information. Monthly burned area data set used in study consists of two products. Burned area from 1901 to 1996 is obtained from Yang *et al.* [2014a], while burned area from 1997 to 2010 is from Global Fire Emissions Database version 3 (GFED3) [Giglio *et al.*, 2010].

The burned area in Yang *et al.* [2014a] is consistent with the long-term trend of global fire activities derived from charcoal records collected across the globe [Marlon *et al.*, 2008]. To the best of our knowledge, this data set [Yang *et al.*, 2014a] is the only available data set providing estimates of monthly global burned area at century-long period and can be used for large-scale ecosystem modeling. Nonetheless, we should be cautious of uncertainties associated with some assumptions in this data set. Human-induced ignitions and suppression strength were parameterized according to population density, which, to some extent, cannot fully represent these stochastic and subjective processes. The input data sets (such as lightning frequency and deforestation rate) to drive the fire model in Yang *et al.* [2014a] also contributed to uncertainties. Since the data set of Yang *et al.* [2014a] was reconstructed based on GFED3 burned area climatology, the two data sets can be connected to each other seamlessly. As indicated by this combined data set, global burned area decreased from $547.24 \times 10^4 \text{ km}^2 \text{ yr}^{-1}$ in 1901 to $324.39 \times 10^4 \text{ km}^2 \text{ yr}^{-1}$ in 2010, with a significant declining trend of $-1.84 \times 10^4 \text{ km}^2 \text{ yr}^{-1}$ (Mann-Kendall trend significance test, P value < 0.05 , same hereafter) (Figure 1).

2.3. Model Implementation and Experimental Design

To investigate fire-induced carbon fluxes, we designed two model experiments, i.e., “fire-on” and “fire-off”. The implementation of the DLEM simulation is composed of three stages: equilibrium run, spin-up,

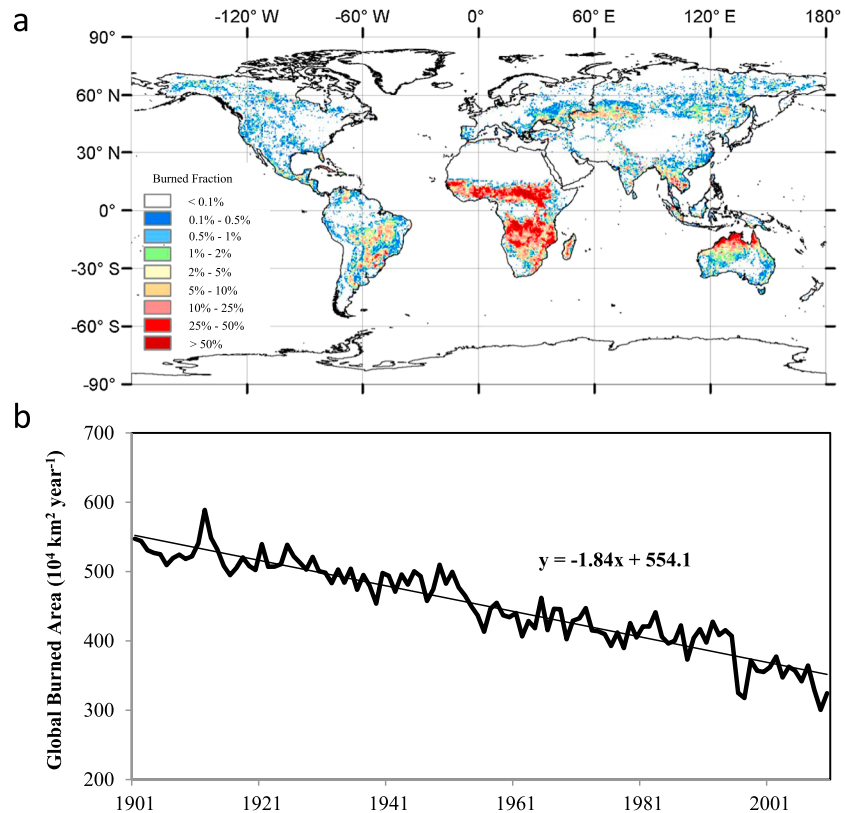


Figure 1. (a) Spatial distribution of global burned fraction (%) and (b) long-term trend and year-to-year variation of global burned area ($10^4 \text{ km}^2 \text{ yr}^{-1}$) during 1901–2010.

and transient run. Equilibrium run aims to determine the initial condition. During equilibrium run, the DLEM was fed with average climate condition from 1901 to 1930 and other input data (atmospheric CO_2 concentration, nitrogen deposition, and land cover) at the level in 1901, while disturbances (such as fires and harvest) were excluded. For each simulation grid, equilibrium state was assumed to be reached when the changes in annual ecosystem carbon, nitrogen, and water pools were less than 0.1 g C m^{-2} , 0.1 g N m^{-2} , and 0.1 mm between two consecutive 50 years. Both “fire-on” and “fire-off” simulations shared the same initial condition. After equilibrium state was reached, model was run for another 100 years for spin-up purpose. During this stage, time series of driving forces were randomly selected within the 30 years from 1901 to 1930, and fire option was switched on in the “fire-on” experiment but closed in the “fire-off” experiment. The different spin-up strategies in “fire-on” and “fire-off” experiments caused different sizes of vegetation and soil organic carbon/nitrogen pools. At last, the DLEM was run in transient mode driven by the time series of all input data sets from 1901 to 2010.

Pyrogenic carbon emissions were estimated in the “fire-on” experiment. Fire influences on net primary productivity (NPP) and ecosystem heterotrophic respiration (R_h) were estimated as the differences between the “fire-on” and “fire-off” simulations. Net ecosystem production (NEP) was defined as the difference between NPP and R_h . Fire influences on NEP (NEP_{fire}) were calculated according to NPP and R_h in the “fire-on” and “fire-off” simulations:

$$\text{NEP}_{\text{fire}} = (\text{NPP}_{\text{fire-on}} - R_{h_{\text{fire-on}}}) - (\text{NPP}_{\text{fire-off}} - R_{h_{\text{fire-off}}}) \quad (3)$$

Net biome production (NBP) was used to investigate the impact of fires on terrestrial carbon sink, which is defined in this study as the difference between NPP and the sum of R_h , pyrogenic carbon emissions (C_{bt}), carbon emissions during crop harvesting (C_{harv}), and biogenic methane emission (C_{CH_4}). Since fire effects

Table 2. The Comparison of the DLEM-Simulated Carbon Fluxes and Vegetation Carbon Storage With Benchmark Data Sets

	Period	DLEM Estimates	Estimates from Benchmark Data Sets	Spatial Pattern Correlation Coefficient
GPP	2000–2009	108.6 Pg C yr ⁻¹	MODIS: 111.58 Pg C yr ⁻¹ [Zhao et al., 2005]	0.836
	1982–2008	105.1 Pg C yr ⁻¹	MTE: 119 Pg C yr ⁻¹ [Jung et al., 2011]	0.829
NPP	2000–2009	55.1 Pg C yr ⁻¹	MODIS: 53.5 Pg C yr ⁻¹ [Zhao and Running, 2010]	0.784
	1982–1999	52.8 Pg C yr ⁻¹	AVHRR: 54.5 Pg C yr ⁻¹ [Nemani et al., 2003]	-
Pyrogenic carbon emissions	1997–2009	2.43 Pg C yr ⁻¹	GFED3.1: 2.0 Pg C yr ⁻¹ [van der Werf et al., 2010]	0.686
	2003–2008	2.46 Pg C yr ⁻¹	GFAS: 2.1 Pg C yr ⁻¹ [Kaiser et al., 2012]	0.607
Vegetation carbon	2000	471.8 Pg C	IPCC Tier-1: 501.6 Pg C [Ruesch and Gibbs, 2008]	0.783

on C_{harv} and C_{CH_4} are negligible compared to its influences on NPP and Rh , we simplified the equation of fire influences on terrestrial carbon sink (NBP_{fire}) as

$$\text{NBP}_{\text{fire}} = (\text{NPP}_{\text{fire-on}} - Rh_{\text{fire-on}} - C_{\text{bt}}) - (\text{NPP}_{\text{fire-off}} - Rh_{\text{fire-off}}) \quad (4)$$

Furthermore, we designed another two simulations, i.e., “without- CO_2 ” and “without-Ndep,” to examine the effects of changes in atmospheric components (CO_2 concentration and nitrogen deposition) on global pyrogenic carbon emissions. In the “without- CO_2 ” (or “without-Ndep”) simulation, model configurations were similar to the “fire-on” experiment, except that the atmospheric CO_2 concentration (or nitrogen deposition) was kept at the level in 1901 throughout the simulation period. The effect of rising CO_2 concentration on pyrogenic carbon emissions was estimated as the differences between the “fire-on” simulation and “without- CO_2 ” simulation. Likewise, the effect of rising nitrogen deposition on pyrogenic carbon emissions was estimated as the differences between the “fire-on” simulation and “without-Ndep” simulation.

2.4. Model Evaluation

The DLEM-simulated gross primary productivity (GPP), NPP, vegetation carbon, and pyrogenic carbon emissions were evaluated against benchmark data sets (Table 2). The spatial distribution of model-simulated GPP was compared with global GPP estimates of Moderate Resolution Imaging Spectroradiometer (MODIS) [Zhao et al., 2005] and empirical-based upscaling product of Multi-Tree Ensemble (MTE) data [Jung et al., 2011], the DLEM-simulated NPP was compared with MODIS and advanced very high resolution radiometer (AVHRR) NPP products [Nemani et al., 2003; Zhao and Running, 2010], the vegetation carbon storage was compared with the Intergovernmental Panel on Climate Change (IPCC) Tier-1 global biomass carbon map [Ruesch and Gibbs, 2008], and the pyrogenic carbon emissions were compared with the estimations of GFED3.1 [van der Werf et al., 2010] and Global Fire Assimilation System (GFAS) [Kaiser et al., 2012]. Availability of these benchmark data sets is described in the supporting information. It is worth noting that all of these benchmarks are model-based results and have their own source of uncertainties. For example, MODIS GPP product was developed based on a light use efficiency model, and the GFED3.1 fire emissions were simulated by the Carnegie-Ames-Stanford Approach model.

The DLEM-simulated GPP and NPP are found to be close to benchmark data sets [Pan et al., 2015]. The global GPP simulated by the DLEM is 2.7% lower than MODIS estimates and 11.7% lower than MTE estimates. The DLEM-simulated global NPP is 3% higher than MODIS estimation and 3.1% lower than AVHRR estimation. The DLEM-simulated global pyrogenic carbon emissions are 21.5% and 17.1% higher than the GFED3.1 and GFAS estimates, respectively. In some regions (such as the continental U.S. and Russia), fire emissions were recognized to be underestimated by the GFED3.1 product [Zhang et al., 2014; Konovalov et al., 2011]. In 2000, the DLEM-simulated global vegetation carbon storage is 471.8 Pg C, which is 5.9% lower than the IPCC Tier-1 result. In general, DLEM-simulated terrestrial CO_2 uptake, pyrogenic carbon emissions, and vegetation carbon storage fall into a reasonable range. The spatial distribution of the DLEM-simulated carbon fluxes and vegetation carbon storage are highly correlated with these benchmark data sets (see Table 2 and Figures S2–S5).

3. Results

3.1. Changing Trend in Pyrogenic Carbon Emissions

From 1901 to 2010, the DLEM-simulated global pyrogenic carbon emissions were $2.43 \pm 0.27 \text{ Pg C yr}^{-1}$ (average ± 1 standard deviation, same hereafter), with the maximum carbon emissions occurred in 1912

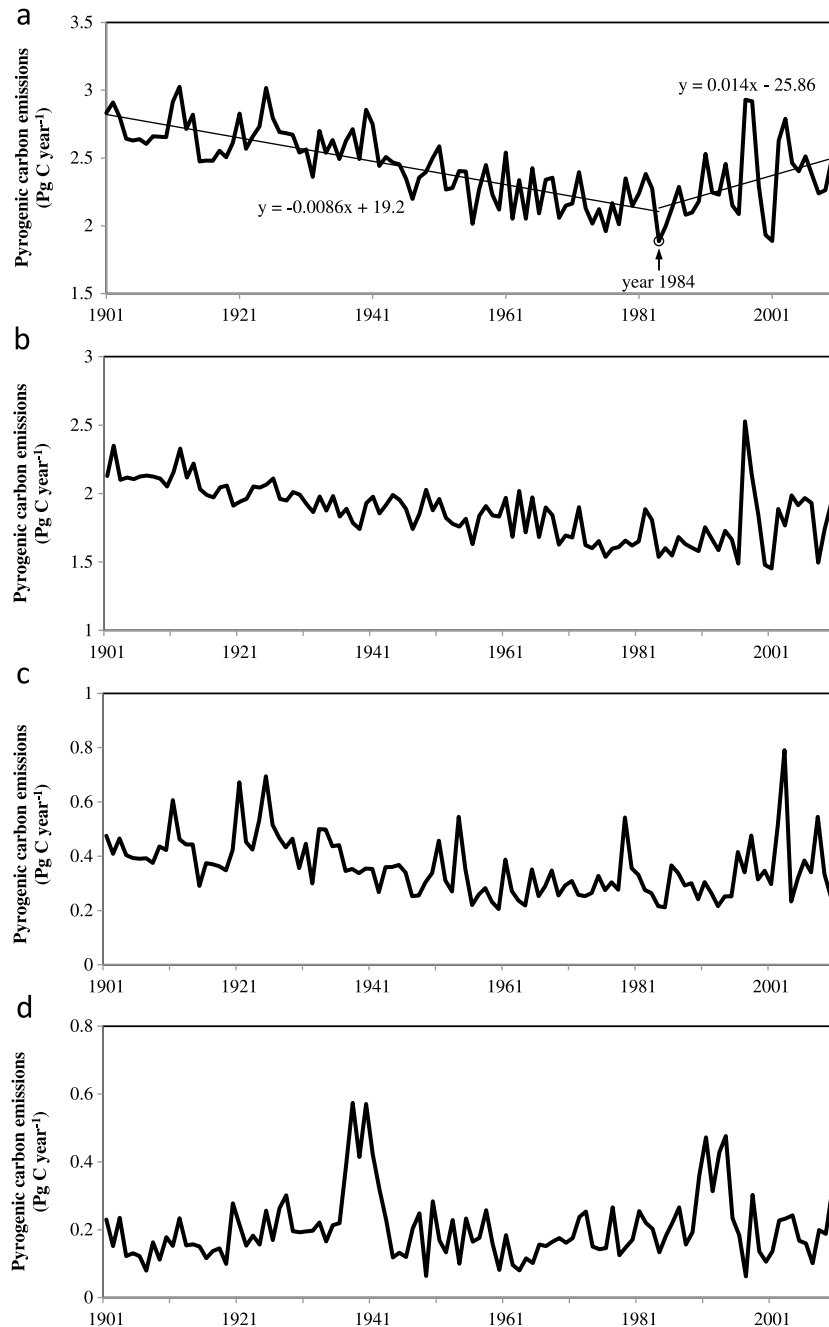


Figure 2. Interannual variations of pyrogenic carbon emissions (Pg C yr^{-1}) from 1901 to 2010 at a (a) global level, in the (b) low latitudes, (c) midlatitudes, and (d) high latitudes.

($3.02 \text{ Pg C yr}^{-1}$). Although global burned area in some other years (such as 1997 and 2009) was even lower, the minimum carbon emissions were found in 2001 ($1.89 \text{ Pg C yr}^{-1}$), which indicates a smaller combustion rate (carbon emissions per unit area burned, in unit g C m^{-2} burned area) in this year. Pyrogenic carbon emissions decreased significantly from the early 20th century to the mid-1980s at a rate of $-0.0086 \text{ Pg C yr}^{-1}$, followed by a significant upward trend at a rate of $0.014 \text{ Pg C yr}^{-1}$ from 1984 to 2010 (Figure 2). The upward trend in pyrogenic carbon emissions since 1984 was mainly contributed by the low latitudes (defined as the region between 30°N and 30°S , increasing rate is $0.011 \text{ Pg C yr}^{-1}$) and midlatitudes (defined as the region between 30°N and 55°N and region between 30°S and 55°S , increasing rate is $0.006 \text{ Pg C yr}^{-1}$). However, the changing trend in pyrogenic carbon emissions in the high latitudes (defined as 55°N and north) was

Table 3. The Statistics of Average Burned Area, Pyrogenic Carbon Emissions, and Combustion Rate From 1901 to 2010 at Global and Continental Scales^a

	Burned Area ($\times 10^4 \text{ km}^2 \text{ yr}^{-1}$)	Pyrogenic Carbon Emissions (Pg C yr^{-1})	Combustion Rate (g C m^{-2} Burned Area)
Globe	451.8	2.43	537.85
Africa	310.8 (68.8%)	1.07 (44%)	344.27
Asia	46.2 (10.2%)	0.48 (19.8%)	1038.96
Oceania	43.3 (9.6%)	0.13 (5.3%)	300.23
South America	36.2 (8%)	0.44 (18.1%)	1215.47
North America	10.2 (2.3%)	0.26 (10.7%)	2549.02
Europe	5.1 (1.1%)	0.05 (2.1%)	980.39

^aThe values within the parentheses denote their contributions to global total amount.

not significant after the 1980s. Our result is similar to *Balshi et al.* [2007], which reported that, in boreal North America (i.e., Canada and Alaska), fire emissions in the 1990s were lower than those in the 1980s.

3.2. Spatial Pattern of Pyrogenic Carbon Emissions

Our results show that about 1.87 ± 0.2 Pg organic carbon was burned annually in the low latitudes, accounting for 77% of the global total amount. Pyrogenic carbon emissions in the midlatitudes and high latitudes accounted for 14.8% and 8.2% of the global total, respectively. At continental level, Africa accounted for 44% of global total pyrogenic carbon emissions, followed by Asia (19.8%), South America (18.1%), North America

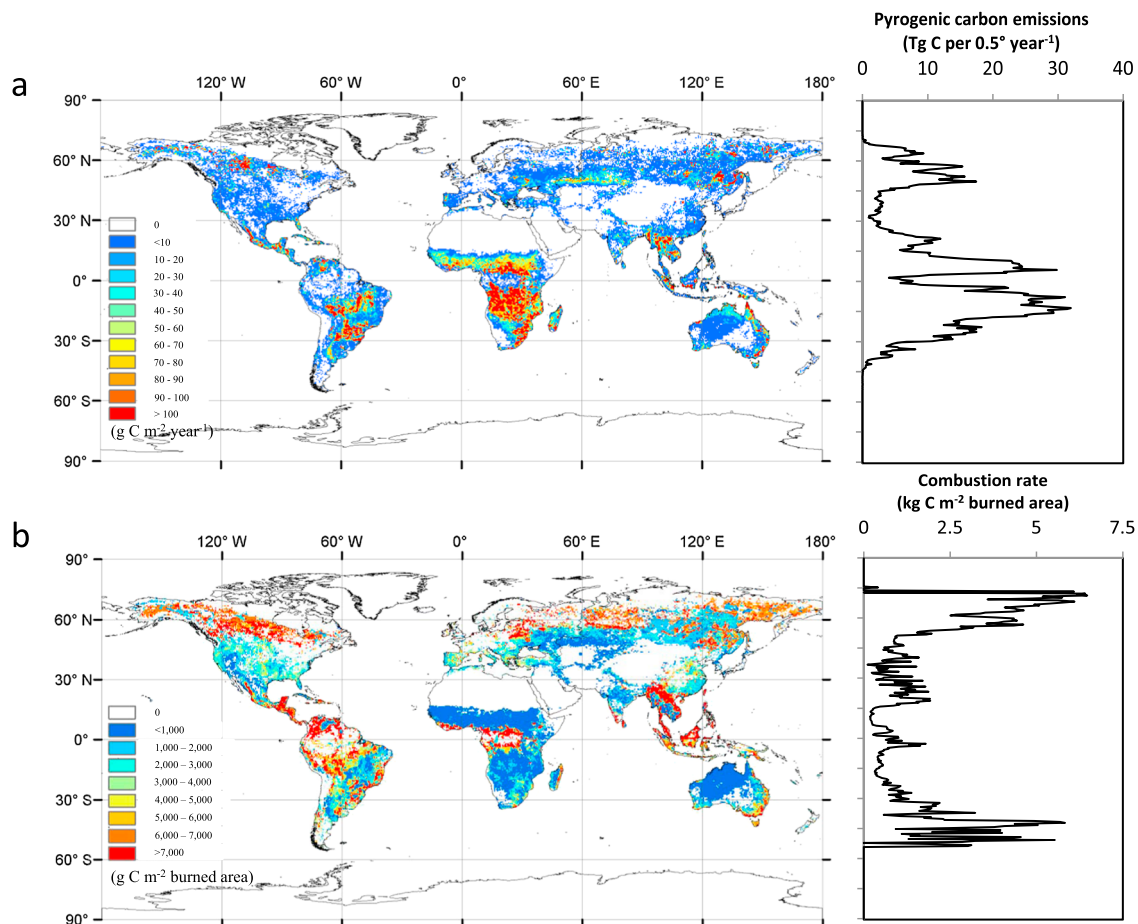


Figure 3. (a) Spatial distribution of the 110 year average pyrogenic carbon emissions ($\text{g C m}^{-2} \text{ yr}^{-1}$) and total carbon emission per 0.5° latitudinal band ($\text{Tg C per } 0.5^\circ \text{ yr}^{-1}$) and (b) combustion rate in area affected by fires (g C m^{-2} burned area) and average combustion rate per 0.5° latitudinal band (kg C m^{-2} burned area).

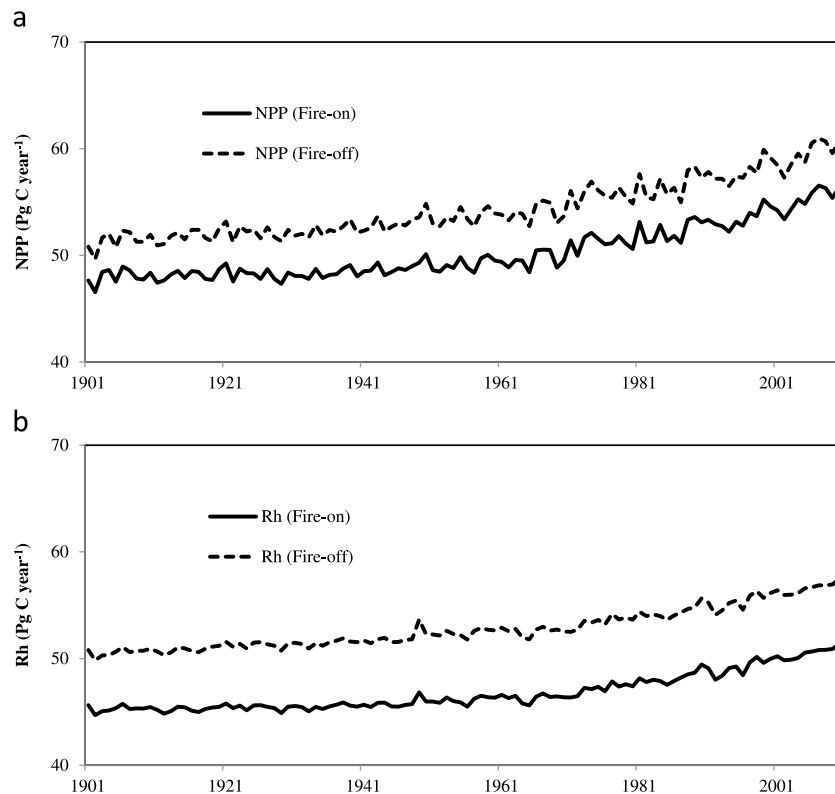


Figure 4. (a) Temporal variations of global net primary productivity (NPP, Pg C yr^{-1}) and (b) heterotrophic respiration (Rh , Pg C yr^{-1}) simulated by the DLEM.

(10.7%), Oceania (5.3%), and Europe (2.1%) (Table 3). The global combustion rate estimated by the DLEM was $537.85 \text{ g C m}^{-2}$ burned area, with the highest in North America ($2549.02 \text{ g C m}^{-2}$ burned area) and the lowest in Oceania ($300.23 \text{ g C m}^{-2}$ burned area). Generally, combustion rate in the pantropical region was lower than that in the pan-boreal region (Figure 3). The differences in combustion rate among regions could be attributed to fuel loading, fire return interval, and vegetation composition. In the tropical savannas, frequent fires reduced fuel loading and then fuel combustion rate, while fires in the boreal forests have a longer return interval and leave sufficient time for forest recovery and fuel accumulation. The prevalent crown fire in the boreal forests may substantially alter vegetation composition and combust more fuels than tropical savanna fires.

3.3. The Role of Fire in the Terrestrial Carbon Budget

The DLEM-simulated global NPP and Rh show continuously increasing trends from 1901 to 2010 as a result of multiple environmental changes (Figure 4). The mean global terrestrial NPP over the entire study period was estimated to be $50.22 \text{ Pg C yr}^{-1}$ and $54.36 \text{ Pg C yr}^{-1}$ in the “fire-on” and “fire-off” simulations, respectively (Figure 4a). Therefore, under the influences of fires, globally, NPP decreased by $4.14 \text{ Pg C yr}^{-1}$, with the largest NPP reduction in Africa ($2.59 \text{ Pg C yr}^{-1}$) (Table 4). NPP reduction in the “fire-on” simulation was primarily

Table 4. The Influences of Fires on Terrestrial Carbon Fluxes and Carbon Budget at Global and Continental Scales During 1901–2010

	NPP Change (Pg C yr^{-1})	Rh Change (Pg C yr^{-1})	NEP Change (Pg C yr^{-1})	NBP Change (Pg C yr^{-1})
Globe	-4.14	-6	1.86	-0.57
Africa	-2.59	-3.49	0.9	-0.17
Asia	-0.5	-0.8	0.3	-0.18
Oceania	-0.24	-0.36	0.12	-0.01
South America	-0.59	-0.97	0.38	-0.06
North America	-0.17	-0.29	0.12	-0.14
Europe	-0.05	-0.09	0.04	-0.01

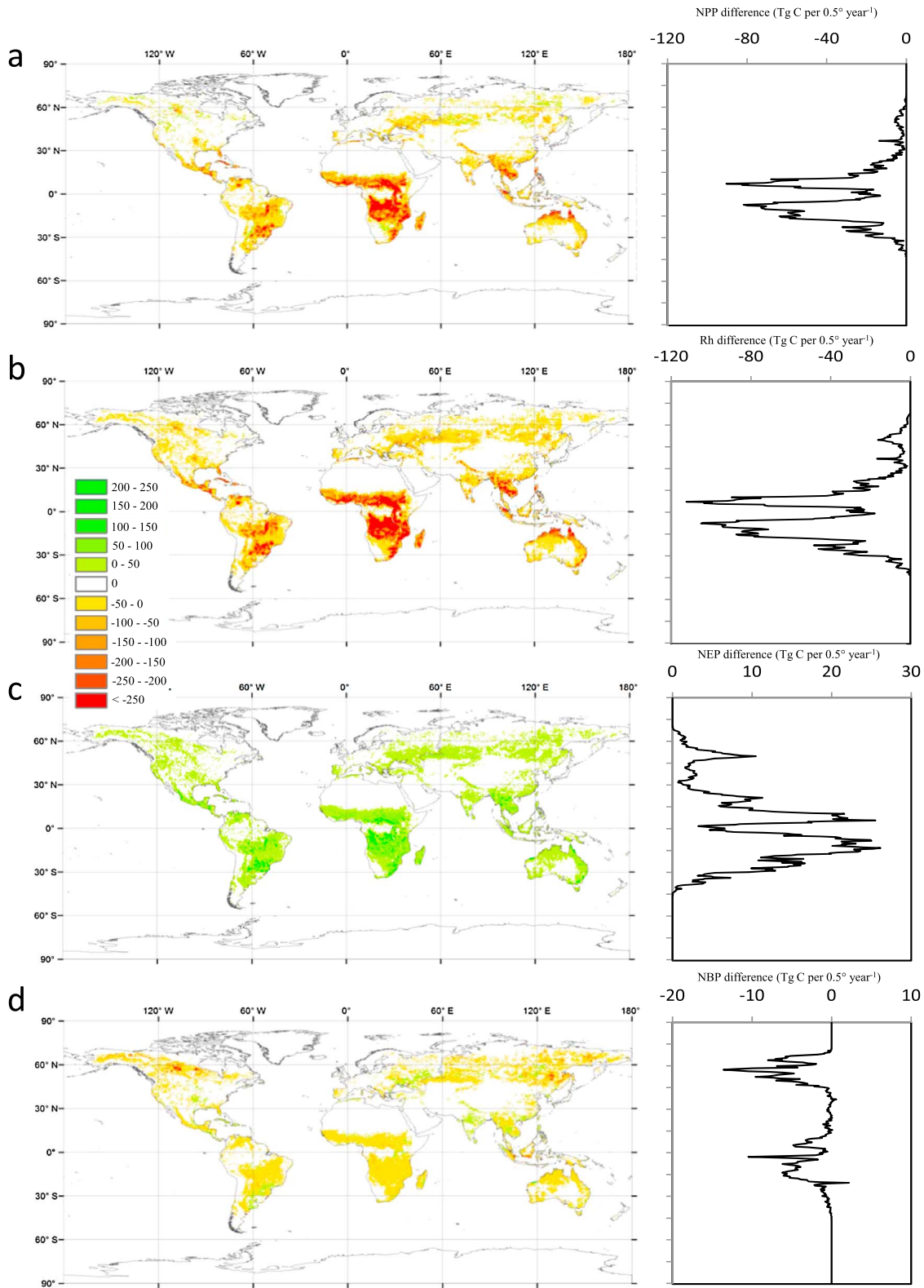


Figure 5. (a) Fire-induced changes in net primary productivity (NPP, $\text{g C m}^{-2} \text{ yr}^{-1}$), (b) heterotrophic respiration (R_h , $\text{g C m}^{-2} \text{ yr}^{-1}$), (c) net ecosystem production (NEP, $\text{g C m}^{-2} \text{ yr}^{-1}$), and (d) net biome production (NBP, $\text{g C m}^{-2} \text{ yr}^{-1}$) and the summation of differences in each 0.5 latitudinal band ($\text{Tg C per } 0.5^\circ \text{ yr}^{-1}$). Differences in the carbon fluxes are calculated by the “fire-on” and “fire-off” simulations.

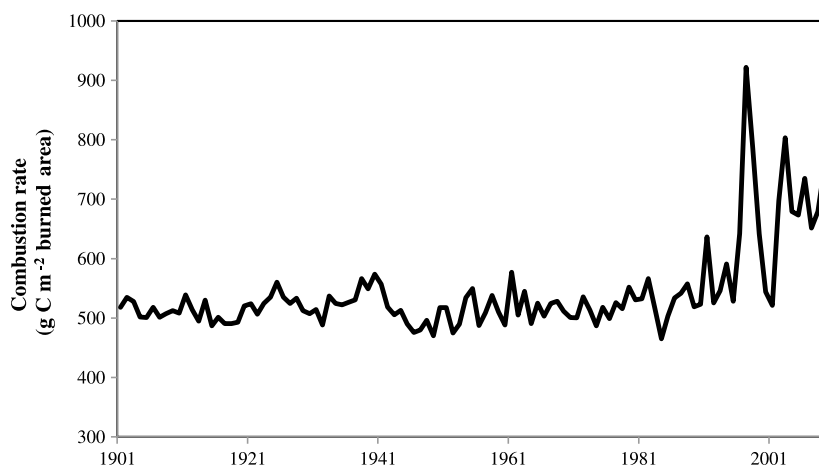


Figure 6. Interannual variations in global average combustion rate (g C m^{-2} burned area) during 1901–2010.

caused by less forest coverage and lower soil fertility. The mean global R_h over the 110 years was estimated to be $46.79 \text{ Pg C yr}^{-1}$ and $52.79 \text{ Pg C yr}^{-1}$ in the “fire-on” and “fire-off” simulations, respectively (Figure 4b). Global R_h was reduced by 6 Pg C yr^{-1} under the effects of fire activities, with the largest reduction in Africa ($3.49 \text{ Pg C yr}^{-1}$). The lower R_h in the “fire-on” simulation could be attributed to the lower amount of litter and soil organic matter for microbial decomposition, which partially offset the reduction in carbon sink caused by pyrogenic carbon emissions [Poulter *et al.*, 2015]. R_h reduction caused by fires was higher than the reduction in NPP. Therefore, global NEP in the “fire-on” simulation was $1.86 \text{ Pg C yr}^{-1}$ higher than that in the “fire-off” simulation. While considering both pyrogenic carbon emissions and fire-induced changes in NPP and R_h , terrestrial carbon sink was reduced by $0.57 \text{ Pg C yr}^{-1}$ under the effects of global fires. Three continents with the largest reduction in terrestrial carbon sink were Asia ($0.18 \text{ Pg C yr}^{-1}$), Africa ($0.17 \text{ Pg C yr}^{-1}$), and North America ($0.14 \text{ Pg C yr}^{-1}$).

Along the latitudinal gradient, fire-induced reductions in NPP and R_h show two peaks, with one peak located between 0°N and 15°N and the other between 0°S and 20°S (Figures 5a and 5b). In the low latitudes, NPP was reduced by $3.92 \text{ Pg C yr}^{-1}$, accounting for 94.7% of global NPP reduction; R_h was reduced by $5.52 \text{ Pg C yr}^{-1}$, accounting for 92% of global R_h reduction. The reductions in NPP and R_h in the middle and high latitudes were much lower than those in the low latitudes. Our results show that fire-induced reduction in carbon sink was mainly contributed by two latitudinal bands, i.e., $46\text{--}70^\circ\text{N}$ latitude band (accounting for 48.1% of global fire-induced NBP reduction) and $10\text{--}20^\circ\text{S}$ latitude band (accounting for 42.1% of global fire-induced NBP reduction) (Figure 5d).

4. Discussions

4.1. Long-Term Trends in Pyrogenic Carbon Emissions During 1901–2010

Previous studies reported that burned area in the tropics and extratropics presented a declining trend in the 20th century [Marlon *et al.*, 2008; Yang *et al.*, 2014a]. In the first decade of the 21st century, satellite observations also found a declining trend in global burned area [Giglio *et al.*, 2013]. Prior to the 1980s, the downward trend in burned area could be the major factor determining the declines in pyrogenic carbon emissions. Human activities, such as fire suppression and cropland expansion, were identified as the main factor controlling the trends in burned area and pyrogenic carbon emissions [Marlon *et al.*, 2008]. However, after the mid-1980s, the trend of pyrogenic carbon emissions reversed, which contradicts the continuously declining trend in burned area. This reversed trend can be explained by a large increase in combustion rate during 1985–2010 (Figure 6), which was mainly caused by the more frequent fires in ecosystems with higher carbon storage (such as tropical rainforest), and the enhanced fuel loading as a result of the rising CO_2 concentration and nitrogen deposition. Our results indicate that average combustion rate during 1985–2010 was $634.74 \text{ g C m}^{-2}$ burned area, compared to $516.38 \text{ g C m}^{-2}$ burned area during 1901–1984.

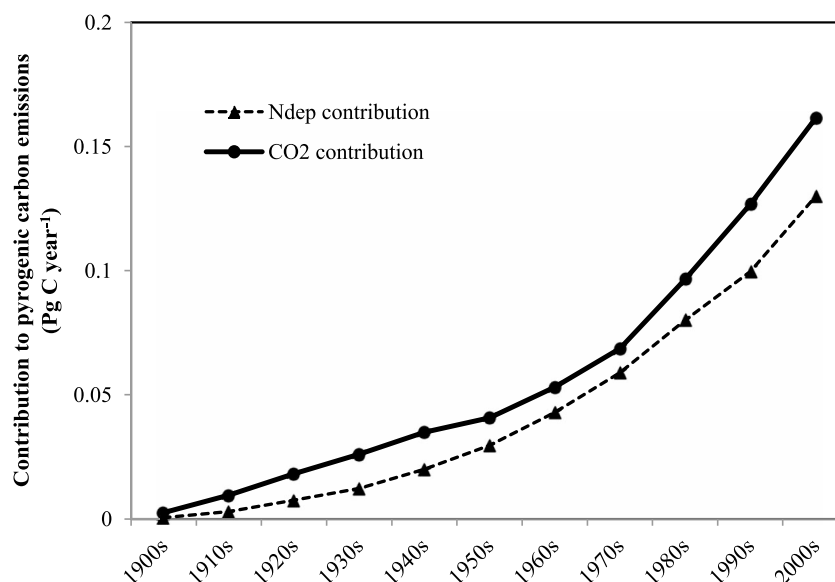


Figure 7. Contributions of atmospheric CO₂ and nitrogen deposition to pyrogenic carbon emissions (Pg C yr⁻¹) from the 1900s to the 2000s.

In recent decades, deforestation has increased rapidly in the tropics. In particular, forest clear-cut area increased from 18,165 km² in 2001 to 23,750 km² in 2004 in Brazilian Amazon basin and increased from 17,000 km² in 1997 to 21,000 km² in 2003 in Indonesia [Santilli *et al.*, 2005]. Fire has been widely used to clear tropical forested land for agricultural cultivation. For deforestation fires, trees are usually reburned several times within 1 year to thoroughly clear the land. Thus, burned area could be several times larger than deforested area, and combustion completeness could be very high [Nepstad *et al.*, 1999]. Since the 1990s, tropical peatland fires have been widely studied. Carbon emissions from deep-burning peatland fires in Indonesia were estimated to be 0.95 Pg C in 1997 and 1998 [Page *et al.*, 2002; van der Werf *et al.*, 2010]. In recent decades, human activities in the Southeast Asia peatlands (such as deforestation, drainage through construction of logging canals, and plantation development) reduced the forest canopy and dried up the fuel, which made peatland soil easier to be ignited [Turetsky *et al.*, 2015; Hooijer *et al.*, 2010]. In the boreal peatlands, recent global warming enhanced fire risk and fire emissions, which resulted in substantial amount of carbon released to the atmosphere. For example, an unprecedented Alaska tundra fire released 2.1 Tg C to the atmosphere in 2007 [Mack *et al.*, 2011].

In many midlatitude regions, burned area showed increasing trend since the 1980s. For example, in the western United States (U.S.), total burned area increased at a rate of 355 km² yr⁻¹ from 1984 to 2011 [Dennison *et al.*, 2014]. The increment in burned area in the western U.S. could be largely attributed to the climate warming, earlier spring, and more frequent droughts [Westerling *et al.*, 2006]. In the early to mid-20th century, fire suppression policies inhibited fire spread and duration [Houghton *et al.*, 2000], which, therefore, enhanced fuel accumulation and induced higher fire emissions in the 21st century. From 1984 to 2012, pyrogenic carbon emissions in conterminous U.S. were reported to be 17.65 ± 12.68 Tg C yr⁻¹ with a significant upward trend at a rate of 0.87 Tg C yr⁻¹. It is worth noting that some regions in the midlatitudes, such as China, experienced continuous declines in burned area and fire emissions from the 1950s to the 2000s due to the intensified fire suppression activities [Lü *et al.*, 2006]. Nevertheless, the declining trend in China did not reverse the overall increasing trend in the entire midlatitudes after the 1980s.

Our input data show that average CO₂ concentration increased from 294.5 ppmv to 393.7 ppmv and average nitrogen deposition rates over land area increased from 0.16 g N m⁻² yr⁻¹ to 0.54 g N m⁻² yr⁻¹ during 1901–2010 (Figure S1). The changes in atmospheric composition have been reported to stimulate terrestrial carbon sequestration and vegetation carbon storage [e.g., Lu *et al.*, 2012; Thomas *et al.*, 2010; Tian *et al.*, 2011; Tian *et al.*, 2012b]. Our further analysis shows that both the changes in CO₂ and nitrogen deposition rates positively contributed to global pyrogenic carbon emissions (Figure 7). Comparing with

1901, the rising CO₂ concentration enhanced global pyrogenic carbon emissions by 0.1 Pg C yr⁻¹, 0.13 Pg C yr⁻¹, and 0.16 Pg C yr⁻¹ in the 1980s, the 1990s, and the 2000s, respectively; the rising nitrogen deposition rates enhanced global pyrogenic carbon emissions by 0.08 Pg C yr⁻¹, 0.1 Pg C yr⁻¹, and 0.13 Pg C yr⁻¹ in the 1980s, the 1990s, and the 2000s, respectively.

4.2. Discrepancy and Consistency in the Estimates of Pyrogenic Carbon Emissions and Fire-Induced Changes in Carbon Sink

The DLEM-simulated global pyrogenic carbon emissions and fire influences on NPP and carbon sink are different from several other model-based estimates, which is mainly caused by different input data and modeling protocols. *Mouillot et al.* [2006] showed that global pyrogenic carbon emissions were 1.5–2.7 Pg C yr⁻¹ at the beginning of the 20th century and increased to 2.7–3.3 Pg C yr⁻¹ by the end of the 20th century. However, our study indicated that global pyrogenic carbon emissions were 2.7 Pg C yr⁻¹ in the 1900s and decreased to 2.36 Pg C yr⁻¹ in the 1990s. This discrepancy could be largely attributed to the difference between global burned area data sets used by *Mouillot et al.* [2006] and this study. The global burned area in *Mouillot et al.* [2006] was $602 \times 10^4 \text{ km}^2 \text{ yr}^{-1}$ during 1997–2000, which is 51.3% higher than GFED3.1 burned area. The declining trend of burned area used in our study is more consistent with global fire history reconstruction according to charcoal records [*Marlon et al.*, 2008]. Nevertheless, both our study and *Mouillot et al.* [2006] show that global pyrogenic carbon emissions presented large increases after the mid-1980s.

The DLEM simulations indicate that fire activities reduced terrestrial carbon sink by 0.57 Pg C yr⁻¹, which is between the estimate of *Li et al.* [2014] (1 Pg C yr⁻¹) and the estimate of *Yue et al.* [2014a] (0.32 Pg C yr⁻¹). The DLEM-simulated global pyrogenic carbon emissions were 2.43 Pg C yr⁻¹, 27.9% higher than those of *Li et al.* [2014] and *Yue et al.* [2014a] (1.9 Pg C yr⁻¹). Both *Li et al.* [2014] and *Yue et al.* [2014a] simulated burned area by fire models, while our study used the satellite-constrained global burned area as input data set to drive the model. It has been recognized that uncertainties in burned area can significantly affect the simulated carbon storage and forest coverage [*Poulter et al.*, 2015].

Large discrepancies exist in the estimates of fire-induced reductions in NPP and *Rh*. *Li et al.* [2014] showed that fire activities reduced global NPP by 1.9 Pg C yr⁻¹, while *Yue et al.* [2014a] found that fire had a negligible effect on NPP reduction. Our study, however, show a fire-induced reduction in NPP by 4.14 Pg C yr⁻¹. Over recent decades, postfire reductions in vegetation biomass and ecosystem productivity have been widely recorded across various climate zones [e.g., *Dore et al.*, 2012; *Hicke et al.*, 2003]. Field fire exclusion experiments [e.g., *Furley et al.*, 2008; *Tilman et al.*, 2000] indicate that fire exclusion can substantially enhance tree coverage and ecosystem carbon storage, which partially supports our argument that tropical savannas have higher NPP in the “fire-off” simulation than in the “fire-on” simulation. Therefore, the reduction in NPP estimated by our study and *Li et al.* [2014] is more reasonable than *Yue et al.* [2014a]. In situ carbon flux measurements are ideal data to validate model results (such as GPP and NEP). Unfortunately, carbon flux measurements in the fire exclusion experiments are still lacking. Nevertheless, *Li et al.* [2014], *Yue et al.* [2014a], and our study agree that fires enlarged global NEP but reduced the size of the terrestrial carbon sink. To identify factors causing these discrepancies and reduce associated uncertainties in simulating fire influences on terrestrial carbon dynamics, it is important to implement an ecosystem-fire model intercomparison with consistent input data including burned area.

4.3. Future Implications

Fire frequencies are projected to increase in many regions across the globe under the impact of climate change throughout the 21st century [*Flannigan et al.*, 2001; *Flannigan et al.*, 2013; *Kloster et al.*, 2012; *Liu et al.*, 2010; *Pechony and Shindell*, 2010]. Many humid regions have contributed to the increases in fire-induced carbon emissions in recent decades (see discussion in section 4.1) and are expected to experience more frequent fires in the future. In the Amazon forests, droughts are projected to be more prevalent, potentially triggering more ignitions [*Phillips et al.*, 2009]. In the historical and contemporary periods, humid interior Amazon forests are less suitable for fire-driven deforestation; however, the percentage of the Amazon basin resistant to deforestation fire is projected to decrease from 58% in contemporary period to 24% in the 2050s [*Le Page et al.*, 2010]. Meanwhile, fires in pan-boreal regions would also be more popular when future climate warming dry up fuel and cause a longer fire season [*Flannigan et al.*, 2009]. In the North America boreal forest, fire-induced carbon emissions were projected to be 2.5–4.4 times their current level by the

end of this century [Balshi *et al.*, 2009]. Once these humid ecosystems (such as tropical humid forests and boreal peatlands) convert to fire-prone systems, regional terrestrial carbon sink would diminish or even become carbon source under the impact of climate warming [Davidson *et al.*, 2012; Turetsky *et al.*, 2002]. For tropical peatlands, human activities facilitated peat ignitions by reducing the coverage of forest canopy [Turetsky *et al.*, 2015]. In the future, peatland protection strategies, such as minimizing forest logging and reducing the rate of cropland expansion, would be of critical importance to mitigating fire-induced carbon emissions as well as enhancing carbon sink on peatlands.

In the 21st century, CO₂ concentration and nitrogen deposition rates are projected to increase continuously [Lamarque *et al.*, 2013; Van Vuuren *et al.*, 2011]. It can be expected that the fertilization effects of increasing CO₂ and nitrogen deposition would continue enhancing ecosystem productivity and promoting fuel accumulation until both elevated CO₂ and nitrogen deposition reach saturation points [Keenan *et al.*, 2011; Pan *et al.*, 2014]. Therefore, future CO₂ and nitrogen deposition would likely lead to higher pyrogenic carbon emissions [Martin Calvo *et al.*, 2014].

4.4. Uncertainties and Improvement Needs

In this study, some uncertainties exist in model parameterization and input data sets, which need to be addressed in the future research. First, in the DLEM, we explicitly considered postfire reduction in forest area and the gradual recovery of tree coverage [Chen *et al.*, 2013] but neglected the growth of herbaceous vegetation in the former forested area. Therefore, ecosystem productivity in the early succession stage might be underestimated. To fully represent postfire trajectories of carbon storage and fluxes, vegetation succession processes and the dynamics of both canopy and understory layers should be considered.

Second, we used burned area as input data, in which satellite information is combined, to drive the DLEM. This method enhanced the model's capacity to simulate both temporal and spatial patterns of burned area. However, it excludes the feedback of ecosystems to fire and may bring some uncertainties into the simulated carbon fluxes and storage.

Third, we used vegetation specific parameters to identify burn severity (combustion completeness and forest mortality), which disregarded the impacts of topography, vegetation species, and weather conditions on burn severity. Field measurements showed that combustion completeness and tree mortality highly depend on local topography, climate/weather condition, and vegetation species [Rogers *et al.*, 2015; van Leeuwen *et al.*, 2014]. Differenced Normalized Burned Ratio (dNBR) is a satellite-based burned severity index, which was found to be in good correlation with ground-based Composite Burn Index in many regions [e.g., Cocke *et al.*, 2005; Miller and Thode, 2007]. Regional and global dNBR data sets have been developed based on MODIS and Landsat images [Loboda *et al.*, 2007; Eidenshink *et al.*, 2007]. The application of satellite-based dNBR could greatly improve the accuracy of model-based simulation of fire emissions. One recent study identified burn severity level ("unburn to low," "low," "medium," and "high") for each satellite pixel within fire perimeter based on the dNBR index and then coupled these different severity levels into ecosystem model to investigate combustion completeness and fire emissions from 1984 to 2012 in the continental United States. Veraverbeke *et al.* [2015] predicted aboveground and belowground carbon consumption by fires between 2001 and 2012 in Alaska by using empirical models driven by dNBR and other environmental factors. To better represent burn severity and reconstruct fire emissions prior to satellite era, however, it is important to develop prognostic burn severity model by considering fuel characteristics and other environmental factors.

It should be noted that, in this study, the contributions of elevated CO₂ and nitrogen deposition to carbon emissions were estimated via their effects on ecosystem carbon storage and fuel loading. A previous study reported that elevated CO₂ and nitrogen deposition can modify burned area [Yang *et al.*, 2014a], which were not included in this study and need further investigation.

5. Conclusions

This study quantified the magnitude and spatiotemporal patterns of century-scale pyrogenic carbon emissions and the role of fire in the terrestrial carbon budget during 1901–2010 by using a land ecosystem model. The simulated results show a downward trend in global pyrogenic carbon emissions between the early 20th century

and the mid-1980s, followed by an upward trend through 2010. During the study period, global pyrogenic carbon emissions were estimated as $2.43 \text{ Pg C yr}^{-1}$, and terrestrial carbon sink was reduced by $0.57 \text{ Pg C yr}^{-1}$ as a result of fire activities. We acknowledge certain caveats related to the representation of biogeochemical processes in modeling dynamic postfire succession, the temporal and spatial resolution of burned area data sets, and model parameterizations such as fuel combustion completeness and forest mortality. This study provides new insight into fire regimes in response to multiple environmental changes by integrating existing environmental information and current understanding of fire impacts on terrestrial ecosystems. To improve the model simulation of fire impacts on terrestrial carbon dynamics, we encourage implementing an ecosystem-fire model intercomparison with consistent input data including burned area.

Acknowledgments

This work has been supported by NSF/USDA/DOE Decadal and Regional Climate Prediction using Earth System Models (NSF1243232, NSF1243220, and NIFC2013-35100-20516), USDA/USDI Joint Fire Science Program (JFSP 11172), and NSF Dynamics of Coupled Natural and Human Systems (1210360). We thank the GFED developing group (<http://www.globalfiredata.org/>) for their provision of global satellite-based fire products. We appreciate the comments from Shree Dargal and contributions of other DLEM developers. We also thank the anonymous reviewers for their valuable comments. The availability of model driving forces and benchmark data is described in the supporting information.

References

- Andela, N., and G. R. van der Werf (2014), Recent trends in African fires driven by cropland expansion and El Niño to La Niña transition, *Nat. Clim. Change*, *4*(9), 791–795.
- Balshi, M. S., et al. (2007), The role of historical fire disturbance in the carbon dynamics of the pan-boreal region: A process-based analysis, *J. Geophys. Res.*, *112*, G02029, doi:10.1029/2006JG000380.
- Balshi, M., A. McGuire, P. Duffy, M. Flannigan, D. Kicklighter, and J. Melillo (2009), Vulnerability of carbon storage in North American boreal forests to wildfires during the 21st century, *Global Change Biol.*, *15*(6), 1491–1510.
- Bond, W., F. Woodward, and G. Midgley (2005), The global distribution of ecosystems in a world without fire, *New Phytol.*, *165*(2), 525–538.
- Bond-Lamberty, B., S. D. Peckham, D. E. Ahl, and S. T. Gower (2007), Fire as the dominant driver of central Canadian boreal forest carbon balance, *Nature*, *450*(7166), 89–92.
- Bousquet, P., P. Ciais, J. Miller, E. Dlugokencky, D. Hauglustaine, C. Prigent, G. R. van der Werf, P. Peylin, E.-G. Brunke, and C. Carouge (2006), Contribution of anthropogenic and natural sources to atmospheric methane variability, *Nature*, *443*(7110), 439–443.
- Bowman, D., and W. Panton (1995), Munmarlary revisited: Response of a north Australian Eucalyptus tetrodonta savanna protected from fire for 20 years, *Aust. J. Ecol.*, *20*(4), 526–531.
- Bowman, D. M., J. K. Balch, P. Artaxo, W. J. Bond, J. M. Carlson, M. A. Cochrane, C. M. D'Antonio, R. S. DeFries, J. C. Doyle, and S. P. Harrison (2009), Fire in the Earth system, *Science*, *324*(5926), 481–484.
- Chen, G., H. Tian, C. Zhang, M. Liu, W. Ren, W. Zhu, A. H. Chappellka, S. A. Prior, and G. B. Lockaby (2012), Drought in the Southern United States over the 20th century: Variability and its impacts on terrestrial ecosystem productivity and carbon storage, *Clim. Change*, *114*(2), 379–397.
- Chen, G., H. Tian, C. Huang, S. A. Prior, and S. Pan (2013), Integrating a process-based ecosystem model with Landsat imagery to assess impacts of forest disturbance on terrestrial carbon dynamics: Case studies in Alabama and Mississippi, *J. Geophys. Res. Biogeosci.*, *118*, 1208–1224, doi:10.1002/jgrg.20098.
- Cocke, A. E., P. Z. Fulé, and J. E. Crouse (2005), Comparison of burn severity assessments using Differenced Normalized Burn Ratio and ground data, *Int. J. Wildland Fire*, *14*(2), 189–198.
- Davidson, E. A., A. C. de Araújo, P. Artaxo, J. K. Balch, I. F. Brown, M. M. Bustamante, M. T. Coe, R. S. DeFries, M. Keller, and M. Longo (2012), The Amazon basin in transition, *Nature*, *481*(7381), 321–328.
- Dennison, P. E., S. C. Brewer, J. D. Arnold, and M. A. Moritz (2014), Large wildfire trends in the western United States, 1984–2011, *Geophys. Res. Lett.*, *41*, 2928–2933, doi:10.1002/2014GL059576.
- Dore, S., M. Montes-Helu, S. C. Hart, B. A. Hungate, G. W. Koch, J. B. Moon, A. J. Finkral, and T. E. Kolb (2012), Recovery of ponderosa pine ecosystem carbon and water fluxes from thinning and stand-replacing fire, *Global Change Biol.*, *18*(10), 3171–3185.
- Eidenshink, J., B. Schwind, K. Brewer, Z. Zhu, B. Quayle, and S. Howard (2007), Project for monitoring trends in burn severity, *Fire Ecol.*, *3*(1), 3–21.
- Flannigan, M. D., M. A. Krawchuk, W. J. de Groot, B. M. Wotton, and L. M. Gowman (2009), Implications of changing climate for global wildland fire, *Int. J. Wildland Fire*, *18*(5), 483–507.
- Flannigan, M., I. Campbell, M. Wotton, C. Carcaillet, P. Richard, and Y. Bergeron (2001), Future fire in Canada's boreal forest: Paleocology results and general circulation model-regional climate model simulations, *Can. J. For. Res.*, *31*(5), 854–864.
- Flannigan, M., A. S. Cantin, W. J. de Groot, M. Wotton, A. Newbery, and L. M. Gowman (2013), Global wildland fire season severity in the 21st century, *For. Ecol. Manage.*, *294*, 54–61.
- Furley, P. A., R. M. Rees, C. M. Ryan, and G. Saiz (2008), Savanna burning and the assessment of long-term fire experiments with particular reference to Zimbabwe, *Prog. Phys. Geogr.*, *32*(6), 611–634.
- Gatti, L., M. Gloor, J. Miller, C. Doughty, Y. Malhi, L. Domingues, L. Basso, A. Martinewski, C. Correia, and V. Borges (2014), Drought sensitivity of Amazonian carbon balance revealed by atmospheric measurements, *Nature*, *506*(7486), 76–80.
- Giglio, L., J. Randerson, G. van der Werf, P. Kasibhatla, G. Collatz, D. Morton, and R. DeFries (2010), Assessing variability and long-term trends in burned area by merging multiple satellite fire products, *Biogeosciences*, *7*(3).
- Giglio, L., J. T. Randerson, and G. R. Werf (2013), Analysis of daily, monthly, and annual burned area using the fourth-generation Global Fire Emissions Database (GFED4), *J. Geophys. Res. Biogeosci.*, *118*, 317–328, doi:10.1002/jgrg.20042.
- Hayes, D., A. McGuire, D. Kicklighter, K. Gurney, T. Burnside, and J. Melillo (2011), Is the northern high-latitude land-based CO₂ sink weakening?, *Global Biogeochem. Cycles*, *25*, GB3018, doi:10.1029/2010GB003813.
- Hicke, J. A., G. P. Asner, E. S. Kasischke, N. H. French, J. T. Randerson, G. James Collatz, B. J. Stocks, C. J. Tucker, S. O. Los, and C. B. Field (2003), Postfire response of North American boreal forest net primary productivity analyzed with satellite observations, *Global Change Biol.*, *9*(8), 1145–1157.
- Hooijer, A., S. Page, J. Canadell, M. Silvius, J. Kwadijk, H. Wösten, and J. Jauhiainen (2010), Current and future CO₂ emissions from drained peatlands in Southeast Asia, *Biogeosciences*, *7*, 1505–1514.
- Houghton, R., J. Hackler, and K. Lawrence (2000), Changes in terrestrial carbon storage in the United States. 2: The role of fire and fire management, *Global Ecol. Biogeogr.*, *9*(2), 145–170.
- Jin, Y., J. T. Randerson, S. J. Goetz, P. S. Beck, M. M. Lorant, and M. L. Goulden (2012), The influence of burn severity on postfire vegetation recovery and albedo change during early succession in North American boreal forests, *J. Geophys. Res.*, *117*, G01036, doi:10.1029/2011JG001886.
- Jung, M., M. Reichstein, H. A. Margolis, A. Cescatti, A. D. Richardson, M. A. Arain, A. Arneeth, C. Bernhofer, D. Bonal, and J. Chen (2011), Global patterns of land-atmosphere fluxes of carbon dioxide, latent heat, and sensible heat derived from eddy covariance, satellite, and meteorological observations, *J. Geophys. Res.*, *116*, G00J07, doi:10.1029/2010JG001566.

- Kaiser, J., A. Heil, M. Andreae, A. Benedetti, N. Chubarova, L. Jones, J.-J. Morcrette, M. Razinger, M. Schultz, and M. Suttie (2012), Biomass burning emissions estimated with a global fire assimilation system based on observed fire radiative power, *Biogeosciences*, *9*(1), 527–554.
- Kasischke, E. S., and M. R. Turetsky (2006), Recent changes in the fire regime across the North American boreal region—Spatial and temporal patterns of burning across Canada and Alaska, *Geophys. Res. Lett.*, *33*, L09703, doi:10.1029/2006GL025677.
- Keenan, T., J. Maria Serra, F. Lloret, M. Ninyerola, and S. Sabate (2011), Predicting the future of forests in the Mediterranean under climate change, with niche- and process-based models: CO₂ matters!, *Global Change Biol.*, *17*(1), 565–579.
- Kloster, S., N. Mahowald, J. Randerson, and P. Lawrence (2012), The impacts of climate, land use, and demography on fires during the 21st century simulated by CLM-CN, *Biogeosciences*, *9*(1), 509–525.
- Konovalov, I. B., M. Beekmann, I. N. Kuznetsova, A. Yurova, and A. M. Zvyagintsev (2011), Atmospheric impacts of the 2010 Russian wildfires: Integrating modelling and measurements of an extreme air pollution episode in the Moscow region, *Atmos. Chem. Phys.*, *11*(19), 10,031–10,056.
- Lamarque, J. F., et al. (2013), Multi-model mean nitrogen and sulfur deposition from the Atmospheric Chemistry and Climate Model Intercomparison Project (ACCMIP): Evaluation of historical and projected future changes, *Atmos. Chem. Phys.*, *13*(16), 7997–8018.
- Langmann, B., B. Duncan, C. Textor, J. Trentmann, and G. R. van der Werf (2009), Vegetation fire emissions and their impact on air pollution and climate, *Atmos. Environ.*, *43*(1), 107–116.
- Le Page, Y., G. van der Werf, D. Morton, and J. Pereira (2010), Modeling fire-driven deforestation potential in Amazonia under current and projected climate conditions, *J. Geophys. Res.*, *115*, G03012, doi:10.1029/2009JG001190.
- Le Quééré, C., R. J. Andres, T. Boden, T. Conway, R. Houghton, J. I. House, G. Marland, G. P. Peters, G. van der Werf, and A. Ahlström (2013), The global carbon budget 1959–2011, *Earth Syst. Sci. Data*, *5*(1), 165–185.
- Lehner, B., and P. Döll (2004), Development and validation of a global database of lakes, reservoirs and wetlands, *J. Hydrol.*, *296*(1), 1–22.
- Li, F., X. Zeng, and S. Levis (2012), A process-based fire parameterization of intermediate complexity in a dynamic global vegetation model, *Biogeosciences*, *9*(7), 2761–2780.
- Li, F., B. Bond-Lamberty, and S. Levis (2014), Quantifying the role of fire in the Earth system—Part 2: Impact on the net carbon balance of global terrestrial ecosystems for the 20th century, *Biogeosciences*, *11*(5), 1345–1360.
- Liu, M., H. Tian, Q. Yang, J. Yang, X. Song, S. E. Lohrenz, and W. J. Cai (2013), Long-term trends in evapotranspiration and runoff over the drainage basins of the Gulf of Mexico during 1901–2008, *Water Resour. Res.*, *49*, 1988–2012, doi:10.1002/wrcr.20180.
- Liu, Y. (2005a), Atmospheric response and feedback to radiative forcing from biomass burning in tropical South America, *Agric. For. Meteorol.*, *133*(1), 40–53.
- Liu, Y. (2005b), Enhancement of the 1988 northern U.S. drought due to wildfires, *Geophys. Res. Lett.*, *32*, L10806, doi:10.1029/2005GL022411.
- Liu, Y., J. Stanturf, and S. Goodrick (2010), Trends in global wildfire potential in a changing climate, *For. Ecol. Manage.*, *259*(4), 685–697.
- Loboda, T., K. O'neal, and I. Csiszar (2007), Regionally adaptable dNBR-based algorithm for burned area mapping from MODIS data, *Remote Sens. Environ.*, *109*(4), 429–442.
- Lü, A., H. Tian, M. Liu, J. Liu, and J. M. Melillo (2006), Spatial and temporal patterns of carbon emissions from forest fires in China from 1950 to 2000, *J. Geophys. Res.*, *111*, D05313, doi:10.1029/2005JD006198.
- Lu, C., and H. Tian (2013), Net greenhouse gas balance in response to nitrogen enrichment: Perspectives from a coupled biogeochemical model, *Global Change Biol.*, *19*(2), 571–588.
- Lu, C., H. Tian, M. Liu, W. Ren, X. Xu, G. Chen, and C. Zhang (2012), Effect of nitrogen deposition on China's terrestrial carbon uptake in the context of multifactor environmental changes, *Ecol. Appl.*, *22*(1), 53–75.
- Lyons, E. A., Y. Jin, and J. T. Randerson (2008), Changes in surface albedo after fire in boreal forest ecosystems of interior Alaska assessed using MODIS satellite observations, *J. Geophys. Res.*, *113*, G02012, doi:10.1029/2007JG000606.
- Mack, M. C., M. S. Bret-Harte, T. N. Hollingsworth, R. R. Jandt, E. A. Schuur, G. R. Shaver, and D. L. Verbyla (2011), Carbon loss from an unprecedented Arctic tundra wildfire, *Nature*, *475*(7357), 489–492.
- Marlon, J. R., P. Bartlein, C. Carcaillet, D. Gavin, S. Harrison, P. Higuera, F. Joos, M. Power, and I. Prentice (2008), Climate and human influences on global biomass burning over the past two millennia, *Nat. Geosci.*, *1*(10), 697–702.
- Martin Calvo, M., I. Prentice, and S. Harrison (2014), Climate vs. carbon dioxide controls on biomass burning: A model analysis of the glacial-interglacial contrast, *Biogeosci. Discuss.*, *11*(2), 2569–2593.
- Miller, J. D., and A. E. Thode (2007), Quantifying burn severity in a heterogeneous landscape with a relative version of the delta Normalized Burn Ratio (dNBR), *Remote Sens. Environ.*, *109*(1), 66–80.
- Moreira, A. G. (2000), Effects of fire protection on savanna structure in Central Brazil, *J. Biogeogr.*, *27*(4), 1021–1029.
- Mouillot, F., and C. B. Field (2005), Fire history and the global carbon budget: A 1 × 1 fire history reconstruction for the 20th century, *Global Change Biol.*, *11*(3), 398–420.
- Mouillot, F., A. Narasimha, Y. Balkanski, J. F. Lamarque, and C. B. Field (2006), Global carbon emissions from biomass burning in the 20th century, *Geophys. Res. Lett.*, *33*, L01801, doi:10.1029/2005GL024707.
- Nemani, R. R., C. D. Keeling, H. Hashimoto, W. M. Jolly, S. C. Piper, C. J. Tucker, R. B. Myneni, and S. W. Running (2003), Climate-driven increases in global terrestrial net primary production from 1982 to 1999, *Science*, *300*(5625), 1560–1563.
- Nepstad, D. C., A. Verssimo, A. Alencar, C. Nobre, E. Lima, P. Lefebvre, P. Schlesinger, C. Potter, P. Moutinho, and E. Mendoza (1999), Large-scale impoverishment of Amazonian forests by logging and fire, *Nature*, *398*(6727), 505–508.
- Page, S. E., F. Siegert, J. O. Rieley, H.-D. V. Boehm, A. Jaya, and S. Limin (2002), The amount of carbon released from peat and forest fires in Indonesia during 1997, *Nature*, *420*(6911), 61–65.
- Pan, S., H. Tian, S. R. Dangal, C. Zhang, J. Yang, B. Tao, Z. Ouyang, X. Wang, C. Lu, and W. Ren (2014), Complex spatiotemporal responses of global terrestrial primary production to climate change and increasing atmospheric CO₂ in the 21st century, *PLoS One*, *9*(11), e112810, doi:10.1371/journal.pone.0112810.
- Pan, S., H. Tian, S. R. Dangal, Z. Ouyang, C. Lu, J. Yang, B. Tao, W. Ren, K. Banger, and Q. Yang (2015), Impacts of climate variability and extremes on global net primary production in the first decade of the 21st century, *J. Geogr. Sci.*, *25*(9), 1027–1044.
- Pechony, O., and D. Shindell (2009), Fire parameterization on a global scale, *J. Geophys. Res.*, *114*, D16115, doi:10.1029/2009JD011927.
- Pechony, O., and D. T. Shindell (2010), Driving forces of global wildfires over the past millennium and the forthcoming century, *Proc. Natl. Acad. Sci. U.S.A.*, *107*(45), 19,167–19,170.
- Phillips, O. L., L. E. Aragão, S. L. Lewis, J. B. Fisher, J. Lloyd, G. López-González, Y. Malhi, A. Monteagudo, J. Peacock, and C. A. Quesada (2009), Drought sensitivity of the Amazon rainforest, *Science*, *323*(5919), 1344–1347.
- Poulter, B., D. Frank, P. Ciais, R. B. Myneni, N. Andela, J. Bi, G. Broquet, J. G. Canadell, F. Chevallier, and Y. Y. Liu (2014), Contribution of semi-arid ecosystems to interannual variability of the global carbon cycle, *Nature*, *509*(7502), 600–603.

- Poulter, B., P. Cadule, A. Cheiney, P. Ciais, E. Hodson, P. Peylin, S. Plummer, A. Spessa, S. Saatchi, and C. Yue (2015), Sensitivity of global terrestrial carbon cycle dynamics to variability in satellite-observed burned area, *Global Biogeochem. Cycles*, *29*, 207–222, doi:10.1002/2013GB004655.
- Prentice, I. C., D. I. Kelley, P. N. Foster, P. Friedlingstein, S. P. Harrison, and P. J. Bartlein (2011), Modeling fire and the terrestrial carbon balance, *Global Biogeochem. Cycles*, *25*, GB3005, doi:10.1029/2010GB003906.
- Randerson, J., H. Liu, M. Flanner, S. Chambers, Y. Jin, P. Hess, G. Pfister, M. Mack, K. Treseder, and L. Welp (2006), The impact of boreal forest fire on climate warming, *Science*, *314*(5802), 1130–1132.
- Ren, W., H. Tian, B. Tao, A. Chappelka, G. Sun, C. Lu, M. Liu, G. Chen, and X. Xu (2011), Impacts of tropospheric ozone and climate change on net primary productivity and net carbon exchange of China's forest ecosystems, *Global Ecol. Biogeogr.*, *20*(3), 391–406.
- Rogers, B. M., A. J. Soja, M. L. Goulden, and J. T. Randerson (2015), Influence of tree species on continental differences in boreal fires and climate feedbacks, *Nat. Geosci.*, *8*, 228–234.
- Rogers, B., J. Randerson, and G. Bonan (2013), High-latitude cooling associated with landscape changes from North American boreal forest fires, *Biogeosciences*, *10*(2), 699–718.
- Roy, D. P., L. Boschetti, C. O. Justice, and J. Ju (2008), The collection 5 MODIS burned area product—Global evaluation by comparison with the MODIS active fire product, *Remote Sens. Environ.*, *112*(9), 3690–3707.
- Ruesch, A., and H. Gibbs (2008), New IPCC Tier-1 Global Biomass Carbon Map For the Year 2000, Available online from the Carbon Dioxide Information Analysis Center, Oak Ridge Natl. Lab., Oak Ridge, Tenn. [Available at <http://cdiac.ornl.gov>.]
- Santilli, M., P. Moutinho, S. Schwartzman, D. Nepstad, L. Curran, and C. Nobre (2005), Tropical deforestation and the Kyoto Protocol, *Clim. Change*, *71*(3), 267–276.
- Schultz, M. G., A. Heil, J. J. Hoelzemann, A. Spessa, K. Thonicke, J. G. Goldammer, A. C. Held, J. Pereira, and M. van Het Bolscher (2008), Global wildland fire emissions from 1960 to 2000, *Global Biogeochem. Cycles*, *22*, GB2002, doi:10.1029/2007GB003031.
- Seiler, W., and P. J. Crutzen (1980), Estimates of gross and net fluxes of carbon between the biosphere and the atmosphere from biomass burning, *Clim. Change*, *2*(3), 207–247.
- Tansey, K., J. M. Grégoire, P. Defourny, R. Leigh, J. F. Pekel, E. Van Bogaert, and E. Bartholomé (2008), A new, global, multi-annual (2000–2007) burnt area product at 1 km resolution, *Geophys. Res. Lett.*, *35*, L01401, doi:10.1029/2007GL031567.
- Tao, B., H. Tian, W. Ren, J. Yang, Q. Yang, R. He, W. Cai, and S. Lohrenz (2014), Increasing Mississippi river discharge throughout the 21st century influenced by changes in climate, land use, and atmospheric CO₂, *Geophys. Res. Lett.*, *41*, 4978–4986, doi:10.1002/2014GL060361.
- Thomas, R. Q., C. D. Canham, K. C. Weathers, and C. L. Goodale (2010), Increased tree carbon storage in response to nitrogen deposition in the U.S., *Nat. Geosci.*, *3*(1), 13–17.
- Thonicke, K., A. Spessa, I. Prentice, S. Harrison, L. Dong, and C. Carmona-Moreno (2010), The influence of vegetation, fire spread and fire behaviour on biomass burning and trace gas emissions: Results from a process-based model, *Biogeosciences*, *7*(6), 1991–2011.
- Tian, H., J. Melillo, C. Lu, D. Kicklighter, M. Liu, W. Ren, X. Xu, G. Chen, C. Zhang, and S. Pan (2011), China's terrestrial carbon balance: Contributions from multiple global change factors, *Global Biogeochem. Cycles*, *25*, GB1007, doi:10.1029/2010GB003838.
- Tian, H., G. Chen, C. Zhang, M. Liu, G. Sun, A. Chappelka, W. Ren, X. Xu, C. Lu, and S. Pan (2012a), Century-scale responses of ecosystem carbon storage and flux to multiple environmental changes in the southern United States, *Ecosystems*, *15*(4), 674–694.
- Tian, H., et al. (2012b), Food benefit and climate warming potential of nitrogen fertilizer use in China, *Environ. Res. Lett.*, *7*(4), 044020, doi:10.1088/1748-9326/7/4/044020.
- Tian, H., G. Chen, C. Lu, X. Xu, D. J. Hayes, W. Ren, S. Pan, D. N. Huntzinger, and S. C. Wofsy (2014), North American terrestrial CO₂ uptake largely offset by CH₄ and N₂O emissions: Toward a full accounting of the greenhouse gas budget, *Clim. Change*, *129*(3–4), 413–426.
- Tian, H., et al. (2015), Global methane and nitrous oxide emissions from terrestrial ecosystems due to multiple environmental changes, *Ecosyst. Health Sustainability*, *1*:art4, doi:10.1890/EHS14-0015.1.
- Tilman, D., P. Reich, H. Phillips, M. Menton, A. Patel, E. Vos, D. Peterson, and J. Knops (2000), Fire suppression and ecosystem carbon storage, *Ecology*, *81*(10), 2680–2685.
- Turetsky, M. R., E. S. Kane, J. W. Harden, R. D. Ottmar, K. L. Manies, E. Hoy, and E. S. Kasischke (2011), Recent acceleration of biomass burning and carbon losses in Alaskan forests and peatlands, *Nat. Geosci.*, *4*(1), 27–31.
- Turetsky, M. R., B. Benscoter, S. Page, G. Rein, G. R. van der Werf, and A. Watts (2015), Global vulnerability of peatlands to fire and carbon loss, *Nat. Geosci.*, *8*(1), 11–14.
- Turetsky, M., K. Wieder, L. Halsey, and D. Vitt (2002), Current disturbance and the diminishing peatland carbon sink, *Geophys. Res. Lett.*, *29*(11), 1526, doi:10.1029/2001GL014000.
- van der Werf, G. R., J. T. Randerson, G. J. Collatz, L. Giglio, P. S. Kasibhatla, A. F. Arellano, S. C. Olsen, and E. S. Kasischke (2004), Continental-scale partitioning of fire emissions during the 1997 to 2001 El Niño/La Niña period, *Science*, *303*(5654), 73–76.
- van der Werf, G. R., J. T. Randerson, L. Giglio, N. Gobron, and A. Dolman (2008b), Climate controls on the variability of fires in the tropics and subtropics, *Global Biogeochem. Cycles*, *22*, GB3028, doi:10.1029/2007GB003122.
- van der Werf, G. R., J. T. Randerson, L. Giglio, G. Collatz, M. Mu, P. S. Kasibhatla, D. C. Morton, R. DeFries, Y. V. Jin, and T. T. van Leeuwen (2010), Global fire emissions and the contribution of deforestation, savanna, forest, agricultural, and peat fires (1997–2009), *Atmos. Chem. Phys.*, *10*(23), 11,707–11,735.
- van der Werf, G., J. Dempewolf, S. Trigg, J. Randerson, P. Kasibhatla, L. Giglio, D. Murdiyarso, W. Peters, D. Morton, and G. Collatz (2008a), Climate regulation of fire emissions and deforestation in equatorial Asia, *Proc. Natl. Acad. Sci. U.S.A.*, *105*(51), 20,350–20,355.
- van Leeuwen, T., G. van der Werf, A. Hoffmann, R. Detmers, G. Rücker, N. Frensch, S. Archibald, J. Carvalho Jr., G. Cook, and W. de Groot (2014), Biomass burning fuel consumption rates: A field measurement database, *Biogeosciences*, *11*, 7305–7329.
- Van Vuuren, D. P., J. Edmonds, M. Kainuma, K. Riahi, A. Thomson, K. Hibbard, G. C. Hurtt, T. Kram, V. Krey, and J.-F. Lamarque (2011), The representative concentration pathways: An overview, *Clim. Change*, *109*, 5–31.
- Veraverbeke, S., B. M. Rogers, and J. T. Randerson (2015), Daily burned area and carbon emissions from boreal fires in Alaska, *Biogeosciences*, *12*(11), 3579–3601.
- Ward, D., S. Kloster, N. Mahowald, B. Rogers, J. Randerson, and P. Hess (2012), The changing radiative forcing of fires: Global model estimates for past, present and future, *Atmos. Chem. Phys.*, *12*(22), 10,857–10,886.
- Westerling, A. L., H. G. Hidalgo, D. R. Cayan, and T. W. Swetnam (2006), Warming and earlier spring increase western U.S. forest wildfire activity, *Science*, *313*(5789), 940–943.
- Wiedinmyer, C., S. Akagi, R. J. Yokelson, L. Emmons, J. Al-Saadi, J. Orlando, and A. Soja (2011), The Fire INventory from NCAR (FINN): A high resolution global model to estimate the emissions from open burning, *Geosci. Model Dev.*, *4*, 625–641.
- Yang, J., H. Tian, B. Tao, W. Ren, J. Kush, Y. Liu, and Y. Wang (2014a), Spatial and temporal patterns of global burned area in response to anthropogenic and environmental factors: Reconstructing global fire history for the 20th and early 21st centuries, *J. Geophys. Res.* *Biogeosci.*, *119*, 249–263, doi:10.1002/2013JG002532.

- Yang, Q., H. Tian, X. Li, B. Tao, W. Ren, G. Chen, C. Lu, J. Yang, S. Pan, and K. Banger (2014b), Spatiotemporal patterns of evapotranspiration along the North American east coast as influenced by multiple environmental changes, *Ecohydrology*, doi:10.1002/eco.1538.
- Yu, Z., J. Loisel, D. P. Brosseau, D. W. Beilman, and S. J. Hunt (2010), Global peatland dynamics since the Last Glacial Maximum, *Geophys. Res. Lett.*, *37*, L13402, doi:10.1029/2010GL043584.
- Yue, C., P. Ciais, P. Cadule, K. Thonicke, and T. Van Leeuwen (2014a), Modelling the role of fires in the terrestrial carbon balance by incorporating SPITFIRE into the global vegetation model ORCHIDEE—Part 2: Carbon emissions and the role of fires in the global carbon balance, *Geosci. Model Dev. Discuss.*, *7*(6), 9017–9062.
- Yue, C., et al. (2014b), Modelling the role of fires in the terrestrial carbon balance by incorporating SPITFIRE into the global vegetation model ORCHIDEE—Part 1: Simulating historical global burned area and fire regimes, *Geosci. Model Dev.*, *7*(6), 2747–2767.
- Zhang, X., S. Kondragunta, and D. P. Roy (2014), Interannual variation in biomass burning and fire seasonality derived from Geostationary satellite data across the contiguous United States from 1995 to 2011, *J. Geophys. Res. Biogeosci.*, *119*, 1147–1162, doi:10.1002/2013JG002518.
- Zhao, M., and S. W. Running (2010), Drought-induced reduction in global terrestrial net primary production from 2000 through 2009, *Science*, *329*(5994), 940–943.
- Zhao, M., F. A. Heinsch, R. R. Nemani, and S. W. Running (2005), Improvements of the MODIS terrestrial gross and net primary production global data set, *Remote Sens. Environ.*, *95*(2), 164–176.